Journal of *Marine Science and Engineering*

MDPI

Article

Microbial Mat Dominated by *Amphora* spp. and Their Adaptative Strategies in an Arsenic-Rich Brackish Pond

Eleonora Agostino [1,2,†], Angela Macrì [1,2,†], Vincenzo Zammuto [1,2,*], Michela D'Alessandro [3], Marco Sebastiano Nicolò [1], Salvatore Giacobbe [1] and Concetta Gugliandolo [1,2,*]

[1] Department of Chemical, Biological, Pharmaceutical and Environmental Sciences, University of Messina, Viale Ferdinando Stagno D'Alcontres 31, 98166 Messina, Italy; eleonora.agostino@studenti.unime.it (E.A.); angela.macri@studenti.unime.it (A.M.); salvatore.giacobbe@unime.it (S.G.)
[2] Research Centre for Extreme Environments and Extremophiles, Department of Chemical, Biological, Pharmaceutical and Environmental Sciences, University of Messina, Viale Ferdinando Stagno D'Alcontres 31, 98166 Messina, Italy
[3] National Institute of Oceanography and Applied Geophysics—OGS, Sgonico, 34010 Trieste, Italy; mdalessandro@ogs.it
* Correspondence: vzammuto@unime.it (V.Z.); concetta.gugliandolo@unime.it (C.G.)
† These authors contributed equally to this work.

Abstract: Marine diatoms are essential members of both phytoplankton and phytobenthic communities, able to colonize submerged artificial and natural surfaces, contributing to benthic microbial biomass. Diatoms have developed different adaptative mechanisms to cope with various environmental stresses, including high concentrations of heavy metals. The aim of this study was to investigate the arsenic resistance of diatoms, isolated from microbial mats collected from an arsenic-rich brackish pond (Lake Mergolo della Tonnara, Italy), by evaluating (i) their ability to form biofilms in the presence of arsenite (As^{III}) or arsenate (As^{V}), and (ii) the variations in the photosynthetic pigments' contents (i.e., chlorophyll *a* and *c*) in their biofilms. The mats were dominated by members of the genus *Amphora*, and isolates were affiliated with species of *A. capitellata*, *A. coffeaeformis*, and *A. montana*. The strains grew better in the presence of As^{V} than As^{III}, which is generally less toxic. After seven days of incubation, each strain exhibited a different ability to form biofilms on glass surfaces in the presence of arsenic (25 ppm), with *A. montana* strain 27 being the most effective (86%) in the presence of As^{III}, and *A. coffeaeformis* strain 26 (74%) with As^{V}. Photosynthetic pigment levels (chlorophyll *a* and *c*) differed in each biofilm, being poorly reduced by As^{III} in strain 27, and by As^{V} in strain 26, indicating a species-specific response to arsenic stress. Our results indicated that *Amphora* species thriving in this environment can form biofilms as an As-resistance mechanism, maintain their levels of photosynthetic pigments, and support the functioning of the pond ecosystem, with *A. montana* being favored in the presence of As^{III}, whereas *A. coffeaeformis* 26 in the presence of As^{V}. As producers of biofilms, these strains could be useful to develop new strategies to remediate arsenic pollution.

Keywords: arsenic; biofilm; diatom; microalgal mat; resistance; transitional environment

Citation: Agostino, E.; Macrì, A.; Zammuto, V.; D'Alessandro, M.; Nicolò, M.S.; Giacobbe, S.; Gugliandolo, C. Microbial Mat Dominated by *Amphora* spp. and Their Adaptative Strategies in an Arsenic-Rich Brackish Pond. *J. Mar. Sci. Eng.* **2024**, *12*, 1966. https://doi.org/10.3390/jmse12111966

Academic Editor: Jun Gong

Received: 11 September 2024
Revised: 24 October 2024
Accepted: 26 October 2024
Published: 1 November 2024

1. Introduction

Arsenic, a metalloid of both geogenic and anthropogenic origin, can be found in a variety of environments [1]. In nature, arsenic exists both in organic and inorganic forms; the inorganic forms, such as the trivalent arsenite (As^{III}) or pentavalent arsenate (As^{V}), are more toxic than organic forms [2]. In natural aquatic environments, the most toxic arsenite prevails under anoxic conditions, and arsenate in soils and oxygenated surface waters [3]. In rivers, As-contaminated waters have baseline concentrations ranging between 0.1 and 2.1 μg L^{-1}, with an average of 0.8 μg L^{-1} [4–6]. Naturally occurring arsenic enrichment from hydrothermal or meteoric groundwaters can range from 10 up to 370 μg L^{-1} [7]. High

concentrations of natural arsenic in groundwater pose significant health risks to humans, ranging from skin lesions to cancers affecting the brain, liver, kidney, and stomach [4,5]. Consequently, the presence of arsenic in water frequently restricts its use as a potable water source in several regions worldwide. The European Directive 98/83/EC imposed the limit of arsenic in drinking water to 10 μg L^{-1} [8].

It is well known that microorganisms possess resistance strategies in response to toxic concentrations of heavy metals, including nonspecific and specific mechanisms involved in metabolic and enzymatic processes [9,10]. Metabolic pathways that confer As resistance to microalgae include As^{III} oxidation, reduction of As^{V} to As^{III}, methylation, and further transformation to less toxic organic forms, such as arsenosugars or arsenolipids [11]. Nonspecific mechanisms include sequestration into vacuoles [12,13], cell surface binding, complexation of arsenic with different compounds (i.e., thiolic groups, glutathione, and phytochelatins), and biofilm formation ([13] and references therein [14]). Biofilm formation is a complex process that begins with the adhesion of microbial cells to surfaces, followed by the irreversible attachment stage, biofilm development and maturation, in which cells are embedded in the auto-produced matrix, and finally, the biofilm dispersion, in which cells leave the biofilm structure in order to contaminate other surfaces [15,16]. Microbial biofilms play a crucial role in influencing the flux of nutrients, adapting to continuous environmental changes, favoring tolerance to toxic elements even at high concentrations. Biofilms can evolve into more complex cellular assemblages or microbial mats, often present in the liquid–solid interface of various environments [16–18], including extreme environments, such as hypersaline ponds and hot springs [19].

Transitional environments, such as that of Oliveri-Tindari Lagoon (Northeastern Sicily, Italy), are of great importance from a naturalistic and environmental point of view. Previous multidisciplinary investigations carried out in the Oliveri-Tindari Lagoon (including small coastal ponds, i.e., Lake Verde, Lake Mergolo della Tonnara, Lake Marinello, and Lake Fondo Porto) documented qualitative variations in the composition of biological communities in response to high hydrobiological complexity and trophic-sedimentary changes, and provided important results to promote its environmental protection and conservation [20–24]. The whole transitional system of Oliveri-Tindari Lagoon, which was declared a Regional Nature Reserve in 1998 (D.R. No. 745/44.10/12/98), does not suffer relevant anthropogenic impacts, although it is vulnerable and sensitive to environmental forcing, such as the amount of energy supply and trophic load [25–27]. Nevertheless, in contrast with the status of protected area, toxic elements were detected in the past in all basins, including high concentrations of arsenic [28,29], related both to the presence of rocks enriched in arsenic in the same geological formation [30] and the contamination by seagull droppings in the lagoon [31]. In sediments collected from three brackish ponds in the lagoon, where arsenic was found at very high concentrations (on average, 17.25 mg kg^{-1}), the isolation of bacteria capable of growing in the presence of arsenic suggested that they are involved in the biogeochemical cycle of this metalloid [29]. However, to the best of our knowledge, there are no reports on the ability of microalgae to react with arsenic in this area.

Present investigations, revealing the occurrence of conspicuous microbial mats, at least in a basin (Mergolo della Tonnara Pond), allowed to verify the hypothesis that biofilm formation, protecting microalgal cells by binding arsenic, concomitantly allows them to maintain their photosynthetic potential.

The aim of this study was to investigate the arsenic resistance of diatoms, isolated from microbial mats collected from an arsenic-rich brackish pond (Lake Mergolo della Tonnara, Italy), by evaluating (i) their ability to form biofilms in the presence of arsenite (As^{III}) or arsenate (As^{V}), and (ii) the variations in the photosynthetic pigments' content (i.e., chlorophyll *a* and *c*) in their biofilms.

2. Materials and Methods

2.1. Study Area and Sample Collection

The brackish pond, "Lake Mergolo della Tonnara" (38°08′22″ N; 15°03′08″ E; hereafter LMT), belongs to a system of small coastal ponds forming the Oliveri-Tindari Lagoon (Sicily, Italy) in the Gulf of Patti (Figure 1). The lagoon, whose origin is due to the growth of very dynamic coastal splits, is periodically subject to drastic changes, which, however, have only marginally influenced LMT, whose present-day conformation dates back to the early 19th century [26]. On a pluri-decadal timescale, qualitative and quantitative variations in the biological communities have been documented both in LMT and the whole lagoon, in response to high hydrobiological complexity and trophic-sedimentary changes [24,26].

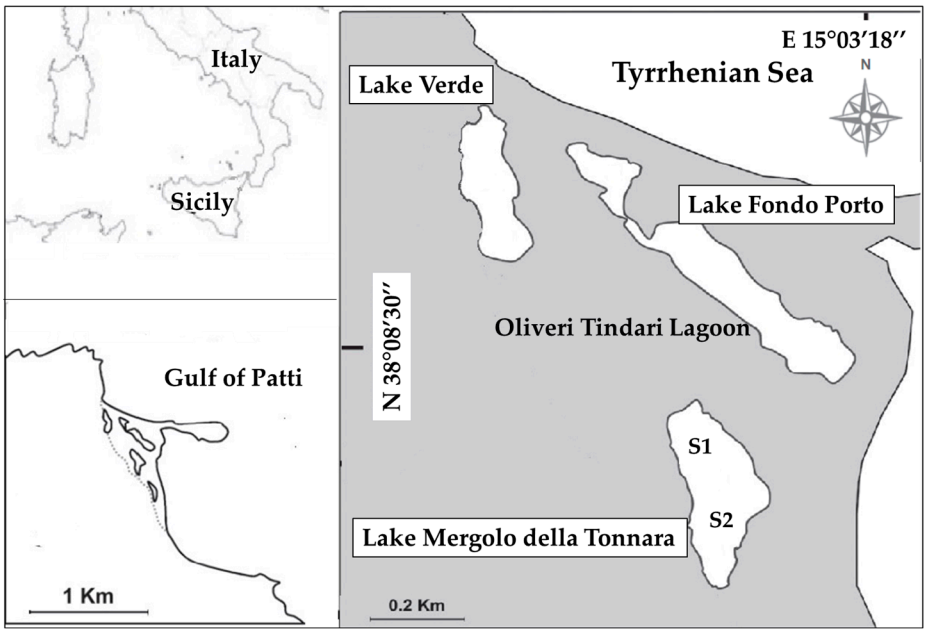

Figure 1. The study area of the Oliveri-Tindari Lagoon (Gulf of Patti, Sicily, Italy) including Lake Verde, Lake Fondo Porto and Lake Mergolo della Tonnara.

In this pond, the temperature, salinity, and pH of bottom water were measured in June 2023 at two sampling stations (S1 and S2), at 3.2 and 3.8 m depths, respectively, using a digital thermometer (Hanna Instrument, Milan, Italy) and Multiparameter Meters (Thermo Scientific™ Orion Star™ A325). Recorded parameters were as follows: temperature 25.4 °C, pH 7.11, salinity 24.5 PSU, and conductibility 38.88 mS cm^{-1} at S1, and temperature 27.9 °C, pH 7.52, salinity 22.3 PSU, and conductibility 37.40 mS cm^{-1} at S2.

Two mat samples (two replicates) were manually collected by a SCUBA diver from the center of the lake (about 3.8 m maximum depth) using sterile polystyrene tubes (50 mL; Thermofisher, Monza, Italy), and they were kept cool in the dark upon arrival at the laboratory.

2.2. Diatom Isolation

The two mat samples were combined and aseptically homogenized by vortexing for 10 min to obtain one representative sample. An aliquot (1 g, *w*/*w*) of the representative mat sample (in triplicate) was suspended in 9 mL of sterile sea water, prefiltered by a sterile 64 µm pore-size cellulose membrane (47 mm in diameter; Millipore, Burlington, MA, USA) to remove higher-size fractions, and each suspension was then filtered by a 3 µm membrane (47 mm in diameter; Millipore) to concentrate the microalgal fraction.

Each membrane filter was seeded on a Guillard f/2 medium agar plate [32] (pH 7.5) incubated at room temperature under continuous illumination (100 µmol of photons m^{-2} s^{-1}) for 7 days. Single colonies were streaked onto f/2 agarose plates until axenic

culture was obtained. Finally, each strain was maintained at room temperature in f/2 broth under continuous insufflation of sterile air (7.2 L min^{-1}).

2.3. Phenotypic and Genotypic Characterization

The isolated strains were observed for cell morphology under light microscopy (Olympus BX60, Tokyo, Japan) and identified according to Sanchez et al. [33].

Cellular lysis and DNA extraction were performed according to the method described by Yuan et al. [34]. Briefly, 2 mL of each culture in stationary phase grown in f/2 broth (OD_{570nm} = 0.5) was centrifuged at 8000× *g* for 10 min, the pellet was resuspended in 50 µL of water PCR reagent (Sigma-Aldrich, Milan, Italy), and 5 sterile silica beads (425–600 µm in diameter; Sigma-Aldrich, Milan, Italy) were added in each tube. The freezing and thawing procedure was applied three times, as follows: 55 °C for 30 min, and then vortexed for 5 min, and placed at −20 °C for 5 min. Each tube was centrifuged at 8000× *g* for 10 min to remove debris, and the supernatant was analyzed using nanodrop (Thermo Scientific™ NanoDrop™, Thermo Fisher Scientific, Wilmington, DE, USA) to quantify DNA and stored at −20 °C.

The 18S rRNA gene was amplified by polymerase chain reaction (PCR) using the My Taq HS DNA Polymerase Kit PCR (Bioline, Camarillo, CA, USA) and the following primers: forward AF (5′ AACCTGGTTGATCCTCCTGCCAG 3′) [35], and reverse: SSUinR1 (5′-CACCAGACTTGCCCCTCCA -3′) [36]. The reaction conditions were 94 °C for 3 min, 40 cycles of 94 °C for 30 s, 55 °C for 30 s, and 72 °C for 1 min, with final extensions of 72 °C for 7 min.

The sequencing of the PCR products was performed by BioFab (Rome, Italy). For microalgae species' identification, a nucleotide BLAST search (http://blast.ncbi.nlm.nih.gov/Blast.cgi) was performed to obtain sequences with the most significant alignment. Sequences assigned to isolates and selected reference sequences were used for phylogenetic tree construction, generated by the neighbor-joining method using the Kimura-2parameters algorithm. Distance matrix trees were generated by the neighbor-joining (NJ) method with the Felsenstein correction, as implemented in the PAUP 4.0B software (Sinauer, Sunderland, MA, USA). The NJ calculation was subjected to bootstrap analysis (1000 replicates).

2.4. Effects of the Presence of As^{III} and As^{V} on Diatoms' Growth

To test the arsenic effects on the growth of the isolates, arsenic was added from filter-sterilized stock solutions of $NaAsO_2$ (As^{III}, pH = 7.2) or Na_2HAsO_4 $7H_2O$ (As^{V}, pH = 6.0) in deionized water at different final concentrations (12.5, 17, 25, and 34 ppm) in f/2 medium. A stationary diatom culture in f/2 after incubation at room temperature was centrifuged at 8000× *g* for 10 min. The diatom pellets (OD_{570nm} = 0.01) were resuspended and inoculated (2 mL) in each tube (18 mL), containing As^{III} or As^{V}, or without As for the control. The tubes were incubated at 25 °C for seven days under 100 µmol photons m^{-2} s^{-1} continuous illumination and atmospheric air insufflation of 7.2 L min^{-1}, and the growth was evaluated spectrophotometrically (OD_{570nm}) after 2, 4, 6, and 7 days.

2.5. Adhesion of Diatoms and Biofilm Formation on the Abiotic Surface in the Presence of As^{III} and As^{V}

Aliquots (27 mL) of each isolated strain in stationary phase culture in f/2 (adjusted to OD_{570nm} = 0.01) were distributed into tubes containing sterile glass slides (25 × 75 mm). After the addition of the As^{III} or As^{V} (3 mL) dissolved in f/2 (sublethal final concentration), the tubes were incubated at room temperature for 7 days under 100 µmol photons m^{-2} s^{-1} illumination. Non-adherent cells on the glass slides were removed by washing five times with sterile PBS; after that, each slide was observed using a light microscope (Olympus BX60, Tokyo, Japan), and the adherent cells were counted. To evaluate the biofilm formation on the glass slides, the extracellular mucopolysaccharides of each biofilm were stained with aqueous Alcian Blue solution (5 mg mL^{-1}, Alcian Blue 8GX, Sigma-Aldrich, Milan, Italy) [37]. The growth of these microalgal biofilms was estimated based on the exopolysaccharide production, highlighted by Alcian Blue staining. The biofilm formation

was expressed as a percentage related to dye intensity present in the microscopic field, evaluated by ImageJ [38] image analysis software. In each experiment, biofilms in triplicates were used for the measurements. To estimate the volume of each biofilm, the ImageJ software (Version 1.54k, USA) plugin, 3D surfaces, was used.

2.6. Photosynthetic Pigments' (Chlorophyll a and c) Concentrations in Biofilms in the Presence of As^{III} or As^{V}

The concentration of the chlorophyll *a* and *c* in each biofilm, formed in the presence or absence of As^{III} or As^{V}, was evaluated according to Zecher et al. [39]. Every two days, one glass slide covered by each biofilm was immersed in the extraction solution of pigments, containing cold acetone (90% *v*/*v*, Sigma-Aldrich, Milan, Italy), for 40 min at room temperature in the dark for up to 7 days. After being centrifuged for 5 min at 1300 rpm, the chlorophyll concentrations were determined spectrophotometrically, as reported by Jeffrey and Humphrey [40]. Briefly, the absorbance at OD = 750 nm, 664 nm, and 630 nm of each supernatant was measured (UV-Vis Spectrophotometer UV-2600, Shimadzu, Duisburg, Germany), and the following equations were used to calculate the total chlorophyll concentrations (μg mL^{-1}):

$$\text{Chl}(a) = 11.47 \times (\text{Abs}_{664\text{nm}} - \text{Abs}_{750\text{nm}}) - 0.4 \times (\text{Abs}_{630\text{nm}} - \text{Abs}_{750\text{nm}}) \quad (1)$$

$$\text{Chl}(c1 + c2) = 24.36 \times (\text{Abs}_{630\text{nm}} - \text{Abs}_{750\text{nm}}) - 3.73 \times (\text{Abs}_{664\text{nm}} - \text{Abs}_{750\text{nm}}) \quad (2)$$

The results were expressed in percentage, as follows:

$$\text{Chl}\% = \text{Chl}_{\text{As}}/\text{Chl}_{\text{control}} \times 100$$

where Chl_{As} is the chlorophyll concentration in the presence of As^{III} or As^{V}, and $\text{Chl}_{\text{control}}$ is that in the absence of As.

2.7. Statistical Analysis

Averages and standard deviations of the experiments carried out in triplicates were used to compare the different experimental groups. Data were analyzed by two-way ANOVA and Tukey's post hoc analysis (GraphPad Software Inc., La Jolla, CA, USA). Significance was considered relevant at $p \leq 0.05$ or highly significant at $p \leq 0.01$.

3. Results

3.1. Diatom Isolation, Phenotypic and Genotypic Characterization

The isolates formed green-brown colonies after 7 days of incubation at 25 °C under 100 μmol photons m^{-2} s^{-1} illumination. In the bright-field microscope, the cells from each colony possessed the cellular morphology belonging to diatoms: amphoroid, with a dorsiventral shell outline, a linear ventral margin and raphe system, settled near the ventral margin, and their girdle-band was a distinguishing characteristic on the dorsal margin (Figure 2).

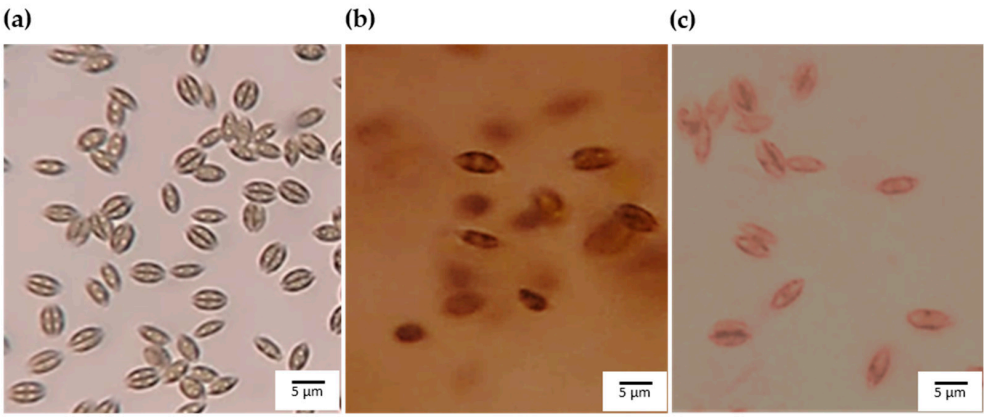

Figure 2. Micrograph of isolated diatoms: (**a**) strain 24, (**b**) strain 26, and (**c**) strain 27 (60×).

The three isolates were phylogenetically attributed to the genus *Amphora* (Table 1). The partial 18S rRNA gene sequences of *Amphora capitellata* 24, *A. coffeaeformis* 26, and *A. montana* 27 were submitted to GenBank.

Table 1. Phylogenetic affiliation, closest sequences, and BLAST similarity (%) of partial 18S rRNA sequences of diatoms isolated from mats of Lake Mergolo della Tonnara.

Strain	Phylogenetic Affiliation	BLAST Similarity (%)	Accession No.
24	*Amphora capitellata* 10S149 isolate D	99.8	JQ886459.1
26	*Amphora coffeaeformis* strain NZmm1W4	100	KY054933.1
27	*Amphora montana* isolate DHmm3W2	100	KU561121.1

3.2. Effects of As^{III} and As^{V} on Diatoms' Growth

The effects of arsenic on the growth of the three strains were evaluated in the presence of As^{III} or As^{V} at different concentrations (12.5, 17, 25, and 34 ppm) after incubation for seven days (Figure 3).

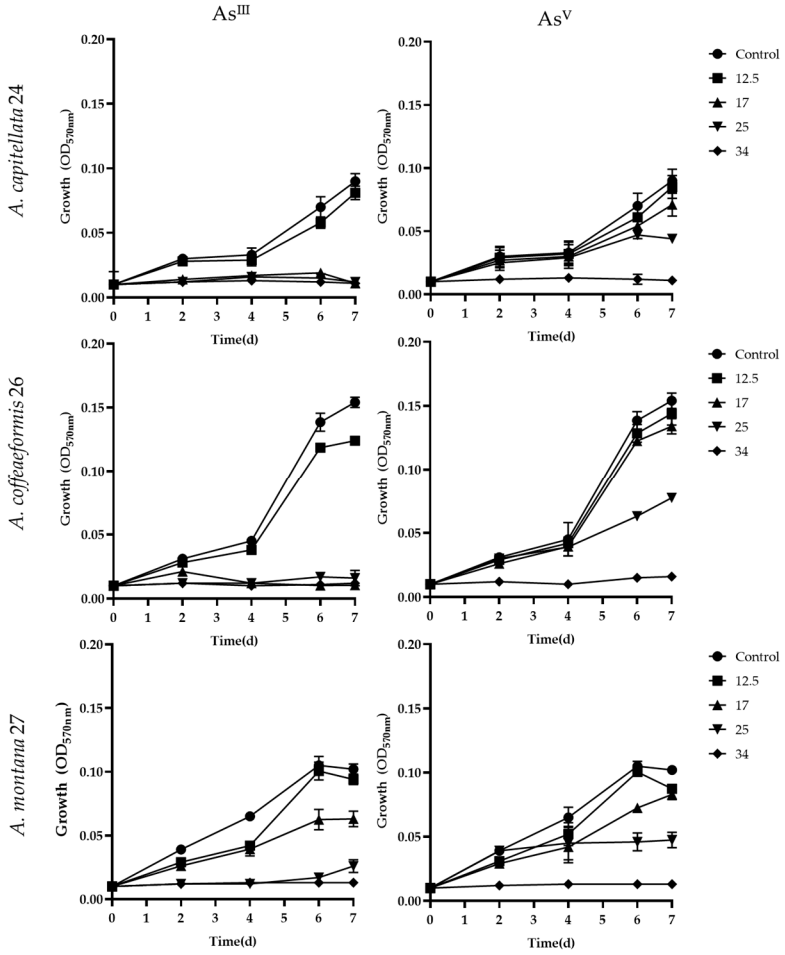

Figure 3. Growth curves of *A. capitellata* 24, *A. coffeaeformis* 26, and *A. montana* 27 in f/2 medium under different concentrations, i.e., 0 (control), 12.5, 17, 25, and 34 ppm of As^{III} or As^{V}. The graphs show data from triplicate experiments (mean ± SD).

In the presence of As^{III}, *A. capitellata* 24 and *A. coffeaeformis* 26 grew up to 12.5 ppm, whereas *A. montana* 27 grew up to 17 ppm, indicating that this strain was the most tolerant to As^{III} (Figure 3). In the presence of As^{V}, all strains grew up to 25 ppm, and *A. coffeaeformis* 26 possessed the highest values at all concentrations.

The toxicity of As^{III} or As^{V} was determined as the effective concentration at which a 50% reduction in the growth of each strain (EC_{50} value) occurred (Figure 4).

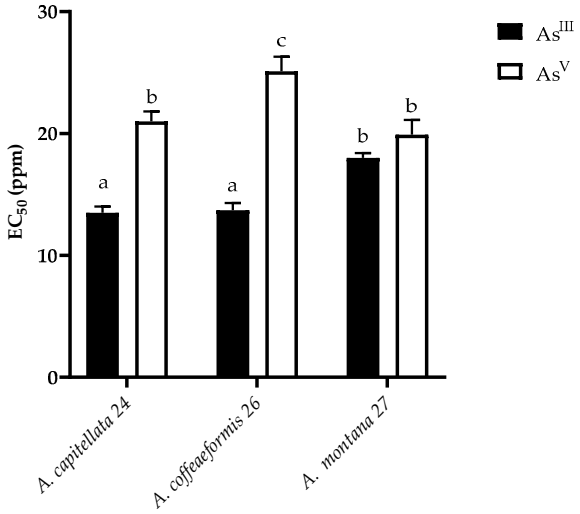

Figure 4. As^{III} (a) or As^{V} (b) (from 12.5 to 34 ppm) toxicity, expressed as EC_{50}, on the viability of *A. capitellata* 24, *A. coffeaeformis* 26, and *A. montana* 27. The bars represent mean ± SD for three replicates (n = 3). Statistical differences were evaluated using two-way ANOVA with Tukey's multiple comparisons tests. Different lowercase letters above the bar graph indicate significant statistical differences ($p \leq 0.05$).

As^{III} toxicity effects were similar for *A. capitellata* 24 and *A. coffeaeformis* 26 (EC_{50} = 13.5 ± 0.5 and 13.7 ± 0.6, respectively), but the toxicity was significantly lower for *A. montana* 27 (EC_{50} = 17.9 ± 0.4). The toxicity of As^{V} was lower than that of As^{III}, with the highest EC_{50} registered for *A. coffeaeformis* 26 (25.1 ± 0.5 ppm), followed by those of *A. capitellata* 24 and *A. montana* 25 (20.8 ± 0.4 and 19.4 ± 0.9 ppm, respectively).

3.3. Effects of As^{III} and As^{V} on Biofilm Formation

The effects of arsenic on the adhesion and biofilm formation by diatoms were investigated at different times, corresponding to the different phases of biofilm formation, i.e., initial attachment (T1), irreversible attachment (T4), and after the biofilm development (T7).

The ability of *Amphora capitellata* 24, *A. coffeaeformis* 26, and *A. montana* 27 to form stable adhesion onto glass surfaces after four days of incubation (T4) in the absence or presence of As^{III} or As^{V} (25 ppm) is shown in Figure 5.

In the presence of As^{III}, *A. montana* 27 (140 ± 2%) was able to adhere onto glass slides more than *A. coffeaeformis* 26 (60 ± 2%) and *A. capitellata* 24 (6 ± 2%). In the presence of As^{V}, the adhesion of *A. coffeaeformis* 26 was the highest (130 ± 2%), followed by *A. capitellata* 24 (86 ± 2%) and *A. montana* 27 (92 ± 2%).

The progression of the biofilm formation, monitored periodically, reflected the same trend as that observed after seven days. After seven days of incubation in the presence of As^{III}, *A. montana* 27 (86 ± 2%) was able to form biofilm on glass slides more than *A. coffeaeformis* 26 (48 ± 2%) and *A. capitellata* 24 (18 ± 1%; Figure 6).

Differently, in the presence of As^{V}, *A. coffeaeformis* 26 formed more biofilm (78 ± 2%) than *A. capitellata* 24 (66 ± 1%) and *A. montana* 27 (62 ± 4%). These results suggest that the cell adhesion and biofilm formation differed in the presence of arsenic in a species-specific manner, with *A. montana* 27 being more effective in the presence of As^{III} and *A. coffeaeformis* 26 in the presence of As^{V} (Figure 7).

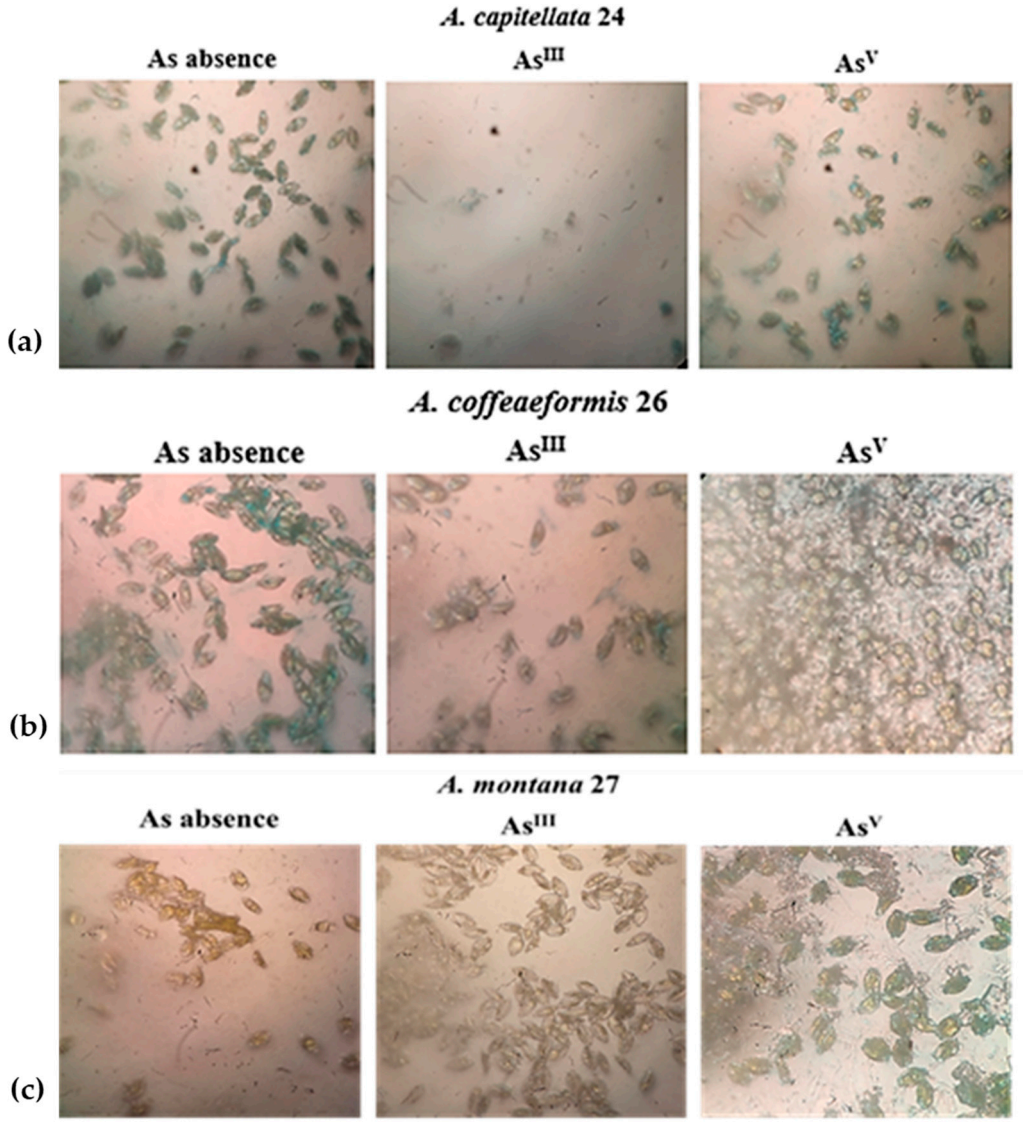

Figure 5. Adhesion of (**a**) *A. capitellata* 24, (**b**) *A. coffeaeformis* 26, and (**c**) *A. montana* 27 onto glass surfaces after four days of incubation in the absence or presence of As^{III} or As^{V} (25 ppm).

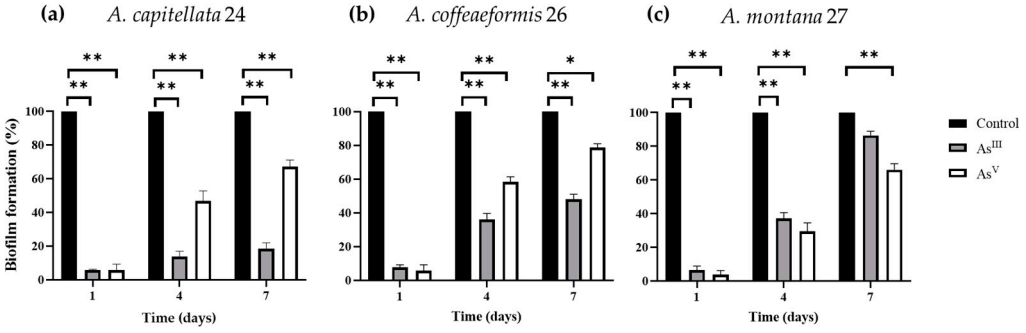

Figure 6. Biofilm formation (%) by *A. capitellata* 24 (**a**), *A. coffeaeformis* 26 (**b**), and *A. montana* 27 (**c**) on glass surfaces in the absence (control) or in the presence of As^{III} or As^{V} (25 ppm) at different times. Statistical differences were evaluated using a two-way ANOVA. * $p \leq 0.05$ and ** $p \leq 0.01$, significant statistical differences compared to the control.

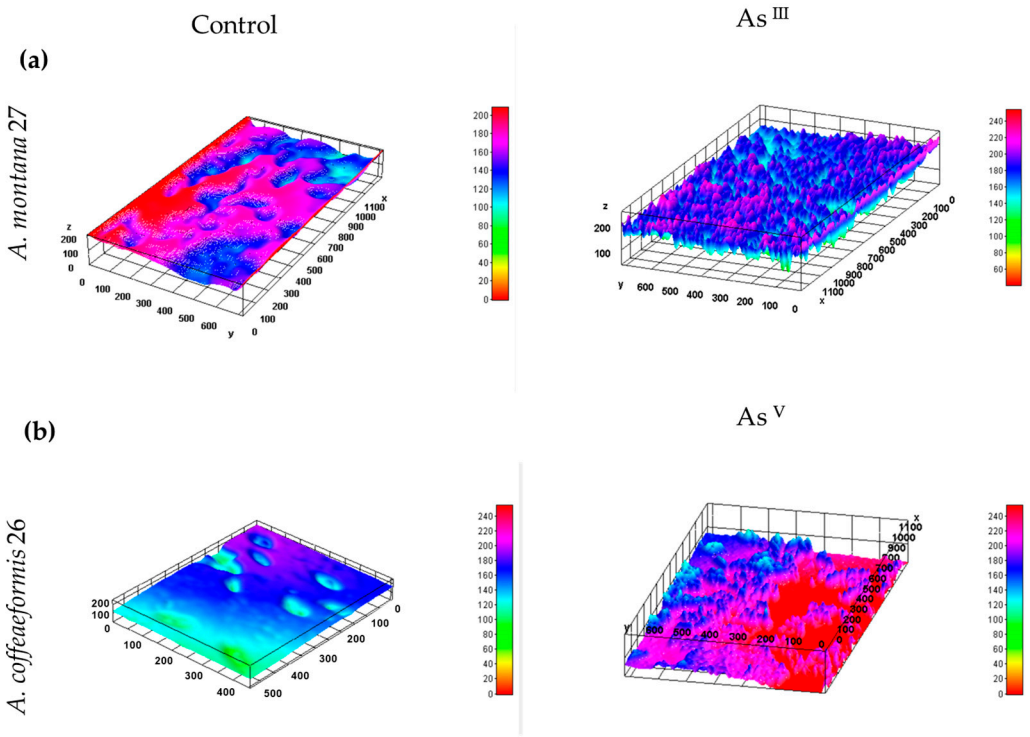

Figure 7. Three-dimensional models of biofilms of the most resistant strains: (**a**) *A. montana* 27 in the absence (control) or presence of As^{III} and (**b**) *A. coffeaeformis* 26 in the absence (control) or presence of As^{V}.

3.4. Photosynthetic Pigments' (Chlorophyll a and c) Concentrations in Biofilms in the Presence of As^{III} and As^{V}

The concentrations of the photosynthetic pigments (chlorophyll *a* and *c*) in the biofilms formed by *A. capitellata* 24, *A. coffeaeformis* 26, and *A. montana* 27 in the presence or absence of As^{III} or As^{V} (25 ppm) are shown in Figures 8 and 9.

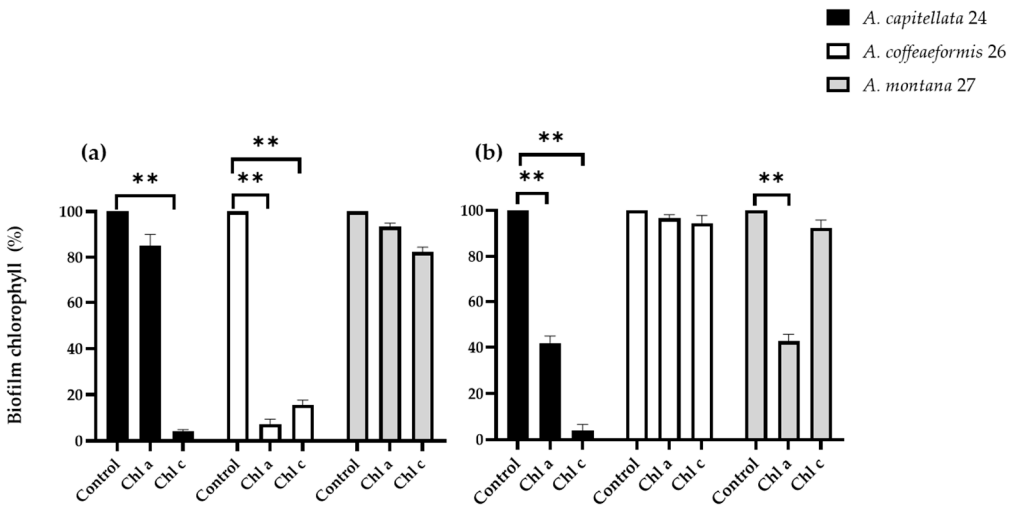

Figure 8. Chlorophyll *a* and chlorophyll *c* content (%) in *A. capitellata* 24, *A. coffeaeformis* 26, and *A. montana* 27 biofilms in the presence or absence of As^{III} (**a**) or As^{V} (**b**), quantified by spectrophotometric analysis. Statistical differences were evaluated using a two-way ANOVA. ** $p \leq 0.01$, significant statistical differences compared to the control.

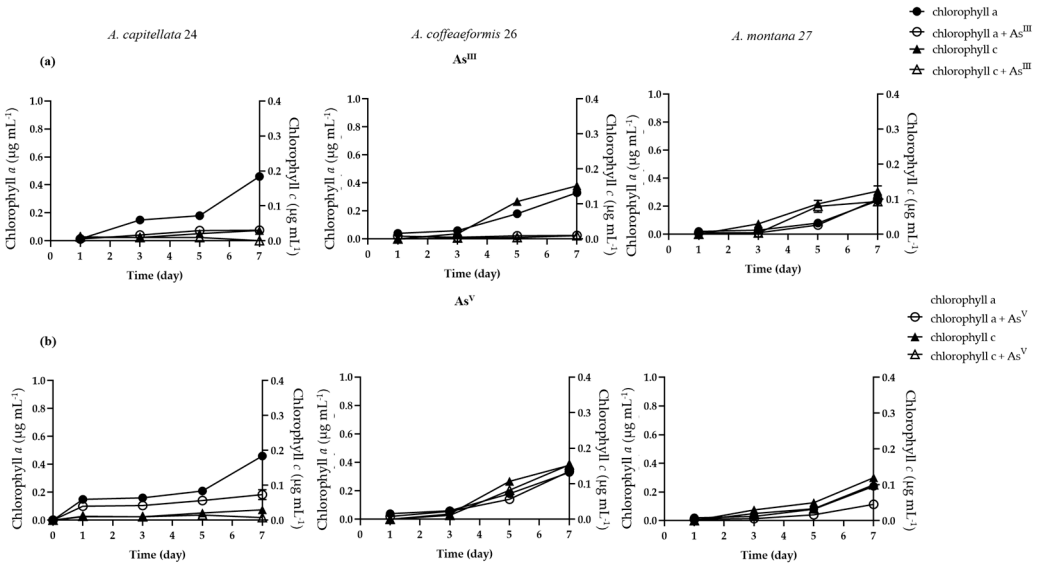

Figure 9. Chlorophyll *a* and chlorophyll *c* concentrations (µg mL^{-1}) in *A. capitellata* 24, *A. coffeaeformis* 26, and *A. montana* 27 biofilms in the presence or absence of As^{III} (**a**) or As^{V} (**b**), quantified by spectrophotometric analysis.

The status of the growth and toxicity of As^{III} and As^{V} could be related to the chlorophyll content during the exposition time (Figure 9).

After seven days of incubation, in the presence of As^{III}, the level of chlorophyll *a* was greatly reduced in *A. coffeaeformis* 26 (92%), followed by *A. capitellata* 24 (85%) and *A. montana* 27 (7.7%; Figures 8a and 9a). Differently, the content of chlorophyll *c* was reduced more in *A. capitellata* 24 (96%) than in *A. coffeaeformis* 26 (85%) and *A. montana* 27 (18%).

In the presence of As^{V}, the level of Chl*a* was poorly affected in the biofilm of *A. coffeaeformis* 26 (3%), whereas it was dramatically reduced in *A. montana* 27 (58%) and in *A. capitellata* 24 (61%). Moreover, the levels of Chl*c* were less affected in the biofilms of *A. coffeaeformis* 26 (6%) and *A. montana* 27 (9%), whereas Chl*c* was greatly reduced in the *A. capitellata* 24 biofilm (97%).

4. Discussion

Exposure to toxicants may alter the physiology and structure of biofilms, leading to changes in ecosystem function and trophic relations. The elevated concentrations of arsenic, mainly of geogenic origin, can lead to heavy metal resistance in the resident microbiota present at the transitional ecosystem of the Lake Mergolo della Tonnara (LMT).

In this study, diatoms that dominated the microbial mats in the salt marsh Lake Mergolo della Tonnara were investigated for their arsenic-adaptative strategies. Toxic effects of arsenic are primarily attributed to the disruption of cell membranes, thereby affecting the uptake of nutrients by attaching themselves to the thiol groups and replacing phosphate ions, which in turn impairs the antioxidant defense mechanisms [41,42] and the energy flux of the photosynthetic machinery [42].

As a result of the microscopic and genotyping characterization, the isolates were affiliated with the genus *Amphora*, and species of *A. capitellata* 24, *A. coffeaeformis* 26, and *A. montana* 27, well-known specialized species able to thrive in hostile environments [43–45]. These three isolates were able to grow better in the presence of arsenate (As^{V}) than arsenite (As^{III}; ranging from 12.5 to 25 µg mL^{-1}), which is the most toxic form. Although the ability to survive different toxic metals, such as nickel, cadmium, chromium, and copper, has been reported for some species of the genus *Amphora* (e.g., *A. coffeaeformis*) [46–48], to our knowledge, only limited information is present for their arsenic resistance.

The production of microbial exopolysaccharides (EPSs), forming complex biofilm structures, contributes to constitutive nonspecific mechanisms involved in the microbial metal resistance or tolerance [49]. In our study, the presence of As forms affected—although at different levels—the ability of the three strains to adhere to, and consequently form biofilms on, glass surfaces, with *A. montana* 27 being the most effective in the presence of As^{III}, and *A. coffeaeformis* 26 the most efficient in the presence of As^{V}. Biofilms produced by the genus *Amphora* (e.g., *A. coffeaeformis* and *A. holsatica*) are notoriously composed mainly (about 90%) of acidic polysaccharides [43], including uronic and glucuronic acids and sulfonic sugars [50–52]. Generally, biosorption occurs via the interaction between negatively charged EPSs and positively charged metal ions (i.e., As, Cu, Pb, and Cd), resulting in their immobilization and, therefore, the inability to penetrate the cell surface [42]. Several types of functional groups in EPSs of diatoms (such as hydroxyl, carboxyl, carbonyl, sulfhydryl, phosphate, and amino groups) could be responsible for the superficial adsorption of arsenic, which plays a significant role in the environmental arsenic detoxification, as also observed by a wide variety of prokaryotes [8].

Although the amounts of EPSs induced by each form of arsenic are not yet known, the presence of acidic residues in the EPSs secreted by the three isolates was corroborated by the ability to adsorb the Alcian Blue dye during biofilm formation, as observed in *A. montana* 27 exposed to As^{III} and in *A. coffeaeformis* 26 in the presence of As^{V} (Figure 5). The high content of uronic acids and pyruvate in the EPSs of *A. coffeaeformis* 26 was previously reported to have adsorptive affinities for certain metal ions (especially copper), as well as high complexation capacities for metal ions, which may, therefore, confer some selective ecological advantages [43]. To our knowledge, this is the first report on the ability of *A. montana* 27 and *A. capitellata* 24 to form biofilms in the presence of arsenic.

The reduction in photosynthetic pigments (Chl*a* and Chl*c*) is considered as the early-warning functional endpoint [53], which is usefully complemented by more structural information for the As damages [53,54]. The presence of As seriously affected the chlorophyll pigment levels in the diatom biofilms due to the substitution of inorganic phosphate by As during the competitive uptake required for both the biosynthesis of pigments and degradation of photosynthetic precursors [42,55]. In the presence of As^{III}, *A. montana* 27 maintained its main photosynthetic pigment (Chl*a*), whereas Chl*c* was moderately reduced, suggesting that the EPSs, as the major components of its biofilm matrix, could hinder the toxic effects of As^{III}. Differently, *A. coffeaeformis* 26 produced the highest amount of biofilms in the presence of the less toxic As^{V}, and it concomitantly maintained the photosynthetic pigment levels, suggesting a protective role of the biofilm matrix against the hazardous effects of As^{V}. Accordingly, EPSs and antioxidant molecules extracted from *A. coffeaeformis* 26 were reported to be able to neutralize the toxic effects in African catfish exposed to As^{V} [55].

The data obtained in this work highlighted the different resistance abilities to arsenic of diatoms from the Lake Mergolo della Tonnara, and suggested that the relative species dominance in the microalgal mats could be induced by the arsenic form present (As^{III} or As^{V}) in the environment, with *A. montana* 27 being favored in the presence of As^{III}, whereas *A. coffeaeformis* 26 in the presence of As^{V}. As biofilm producers in the presence of arsenic, *A. montana* 27 and *A. coffeaeformis* 26 could be further investigated as prospective novel strategies for removing metal ions from polluted environments, as an attractive alternative to the commonly used physicochemical remediation processes.

5. Conclusions

The members of the genus *Amphora*, representing the principal primary producers in the Lake Mergolo della Tonnara, showed species-specific arsenic resistance and adopted biofilm production via secretion of exopolysaccharides as a resistance strategy to cope with As stresses. Moreover, *A. montana* 27 and *A. coffeaeformis* 26, maintaining the levels of the main photosynthetic pigments in the presence of As^{III} or As^{V}, supported the functioning of the pond ecosystem, which can thus be considered a profitable case study of an extreme

environment and related adaptation strategies. These results suggested that, as diatoms well adapted to arsenic, the species of *A. montana* 27 and *A. coffeaeformis* 26 could be considered promising candidates as bioindicators of arsenic-contaminated environments. Finally, as producers of biofilms in arsenic-rich conditions, *A. montana* 27 and *A. coffeaeformis* 26 could be useful to develop novel applications for arsenic bioremediation technologies.

Author Contributions: Conceptualization, E.A., A.M. and V.Z.; methodology, E.A. and M.S.N.; software, A.M.; validation, V.Z., M.D. and S.G.; formal analysis, A.M., E.A. and V.Z.; investigation, E.A. and A.M.; resources, C.G. and S.G.; data curation, C.G. and V.Z.; writing—original draft preparation, E.A.; writing—review and editing, C.G. and S.G.; visualization, V.Z.; supervision, C.G. and S.G.; project administration, C.G.; funding acquisition, C.G. All authors have read and agreed to the published version of the manuscript.

Funding: This work was supported by the project SAMOTHRACE-Sicilian MicronanoTech Research And Innovation Center. European Union—NextGenerationEU (CUP J43C22000310006, SAMOTHRACE—PNRR—Missione 4, Componente 2, Investimento 1.5—ECS00000022).

Institutional Review Board Statement: Not applicable.

Informed Consent Statement: Not applicable.

Data Availability Statement: Data are contained within the article.

Conflicts of Interest: The authors declare no conflicts of interest.

References

1. Garelick, H.; Jones, H.; Dybowska, A.; Valsami-Jones, E. Arsenic Pollution Sources. In *Reviews of Environmental Contamination Arsenic Pollution and Remediation: An International Perspective*; Garelick, H., Jones, H., Eds.; Springer Science & Business Media: New York, NY, USA, 2008; Volume 197, pp. 17–60.
2. Oremland, R.S.; Stolz, J.F. The Ecology of Arsenic. *Science* **2003**, *300*, 939–944. [CrossRef] [PubMed]
3. Shaji, E.; Santosh, M.; Sarath, K.V.; Prakash, P.; Deepchand, V.; Divya, B.V. Arsenic contamination of roundwater: A global synopsis with focus on the Indian Peninsula. *Geosci. Front.* **2021**, *12*, 101079. [CrossRef]
4. Smedley, P.L.; Kinniburgh, D.G. Arsenic in groundwater and the environment. In *Essentials of Medical Geology*; Selinus, O., Ed.; Springer: Dordrecht, The Netherlands, 2013; pp. 279–310.
5. Sharma, V.K.; Sohn, M. Aquatic arsenic: Toxicity, speciation, transformations, and remediation. *Environ. Int.* **2009**, *35*, 743–759. [CrossRef] [PubMed]
6. Casentini, B.; Gallo, M.; Baldi, F. Arsenate and arsenite removal from contaminated water by iron oxides nanoparticles formed inside a bacterial exopolysaccharide. *J. Environ. Chem. Eng.* **2019**, *7*, 102908. [CrossRef]
7. Barral-Fraga, L.; Morin, S.; Rovira, M.D.M.; Urrea, G.; Magellan, K.; Guasch, H. Short-term arsenic exposure reduces diatom cell size in biofilm communities. *Environ. Sci. Pollut. Res.* **2016**, *23*, 4257–4270. [CrossRef]
8. Spanò, A.; Zammuto, V.; Macrì, A.; Agostino, E.; Nicolò, M.S.; Scala, A.; Trombetta, D.; Smeriglio, A.; Ingegneri, M.; Caccamo, M.T.; et al. Arsenic adsorption and toxicity reduction of an exopolysaccharide produced by *Bacillus licheniformis* B3-15 of shallow hydrothermal vent origin. *J. Mar. Sci. Eng.* **2023**, *11*, 325. [CrossRef]
9. Rahman, M.A.; Hasegawa, H.; Lim, R.P. Bioaccumulation, biotransformation and trophic transfer of arsenic in the aquatic food chain. *Environ. Res.* **2012**, *116*, 118–135. [CrossRef]
10. Gupta, P.; Diwan, B. Bacterial Exopolysaccharide mediated heavy metal removal: A review on biosynthesis, mechanism and remediation strategies. *Biotechnol. Rep.* **2017**, *13*, 58–71. [CrossRef]
11. Papry, R.I.; Ishii, K.; Mamun, M.A.A.; Miah, S.; Naito, K.; Mashio, A.S.; Maki, T.; Hasegawa, H. Arsenic biotransformation potential of six marine diatom species: Effect of temperature and salinity. *Sci. Rep.* **2019**, *9*, 10226. [CrossRef]
12. Levy, J.L.; Stauber, J.L.; Adams, M.S.; Maher, W.A.; Kirby, J.K.; Jolley, D.F. Toxicity, biotransformation, and mode of action of arsenic in two freshwater microalgae (*Chlorella* sp. and *Monoraphidium arcuatum*). *Environ. Toxicol. Chem.* **2005**, *24*, 2630–2639. [CrossRef]
13. Olguín, E.J.; Sánchez-Galván, G. Heavy metal removal in phytofiltration and phycoremediation: The need to differentiate between bioadsorption and bioaccumulation. *New Biotechnol.* **2012**, *30*, 3–8. [CrossRef] [PubMed]
14. Wang, N.; Ye, Z.; Huang, L.; Zhang, C.; Guo, Y.; Zhang, W. Arsenic Occurrence and cycling in the aquatic environment: A comparison between freshwater and seawater. *Water* **2022**, *15*, 147. [CrossRef]
15. Monds, R.D.; O'Toole, G.A. The developmental model of microbial biofilms: Ten years of a paradigm up for review. *Trends Microbiol.* **2009**, *17*, 73–87. [CrossRef] [PubMed]
16. Zammuto, V.; Spanò, A.; Agostino, E.; Macrì, A.; De Pasquale, C.; Ferlazzo, G.; Rizzo, M.G.; Nicolò, M.S.; Guglielmino, S.; Gugliandolo, C. Anti-Bacterial adhesion on abiotic and biotic surfaces of the exopolysaccharide from the marine *Bacillus licheniformis* B3-15. *Mar. Drugs* **2023**, *21*, 313. [CrossRef]

17. Bolhuis, H.; Cretoiu, M.S.; Stal, L.J. Molecular ecology of microbial mats. *FEMS Microbiol. Ecol.* **2014**, *90*, 335–350.
18. Magaletti, E.; Urbani, R.; Sist, P.; Ferrari, C.R.; Cicero, A.M. Abundance and chemical characterization of extracellular carbohydrates released by the marine diatom *Cylindrotheca fusiformis* under N- and P-limitation. *Eur. J. Phycol.* **2004**, *39*, 133–142. [CrossRef]
19. Aslam, S.; Cresswell-Maynard, T.; Thomas, D.N.; Underwood, G.J.C. Production and characterization of the intra-and extracellular carbohydrates and polymeric substances (EPS) of three sea-ice diatom species, and evidence for a cryoprotective role for EPS. *J. Phycol.* **2012**, *48*, 1494–1509. [CrossRef]
20. Caruso, A.; Gargano, M.E.; Valenti, D.; Fiasconaro, A.; Spagnolo, B. Cyclic fluctuations, climatic changes and role of noise in planktonic foraminifera in the mediterranean sea. *Fluct. Noise Lett.* **2005**, *5*, 349–355. [CrossRef]
21. Caruso, G.; Leonardi, M.; Monticelli, L.S.; Decembrini, F.; Azzaro, F.; Crisafi, E.; Zappal, G.; Bergamasco, A.; Vizzini, S. Assessment of the ecological status of transitional waters in Sicily (Italy): First characterisation and classification according to a multiparametric approach. *Mar. Pollut. Bull.* **2010**, *60*, 1682–1690. [CrossRef]
22. Leonardi, M.; Azzaro, F.; Azzaro, M.; Decembrini, F.; Monticelli, L. Ciclo della sostanza organica nell'ecosistema lagunare di Tindari (ME) *Biol. Mar. Mediterr.* **2000**, *7*, 222–232.
23. Leonardi, M.; Giacobbe, S. The Oliveri-Tindari Lagoon (Messina, Italy): Evolution of the trophic-sedimentary environment and mollusc communities in the last twenty years. In *Mediterranean Ecosystems*; Faranda, F.M., Guglielmo, L., Spezie, G., Eds.; Springer: Milano, Italy, 2001; pp. 305–310.
24. Mazzola, A.; Bergamasco, A.; Calvo, S.; Caruso, G.; Chemello, R.; Colombo, F.; Giaccone, G.; Gianguzza, P.; Guglielmo, L.; Leonardi, M.; et al. Sicilian transitional waters: Current status and future development. *Chem. Ecol.* **2010**, *26*, 267–283. [CrossRef]
25. Leonardi, M.; Azzaro, F.; Galletta, M.; Giacobbe, M.G.; Masò, M.; Penna, A. Time-series evolution of toxic organisms and related environmental factors in a brackish ecosystem of the Mediterranean Sea. *Hydrobiologia* **2006**, *555*, 299–305. [CrossRef]
26. Leonardi, M.; Bergamasco, A.; Giacobbe, S.; Azzaro, F.; Cosentino, A.; Crupi, A.; Lanza, S.; Randazzo, G.; Crisafi, E. A four decades multiparametric investigation in a Mediterranean dynamic ecosystem: Mollusc assemblages answer to the environmental changes. *Estuar. Coast. Shelf Sci.* **2020**, *234*, 106625. [CrossRef]
27. Signa, G.; Mazzola, A.; Vizzini, S. Effects of a small seagull colony on trophic status and primary production in a mediterranean coastal system (Marinello Ponds, Italy). *Estuar. Coast. Shelf Sci.* **2012**, *111*, 27–34. [CrossRef]
28. Ruta, M.; Pepi, M.; Franchi, E.; Renzi, M.; Volterrani, M.; Perra, G.; Guerranti, C.; Zanini, A.; Focardi, S.E. Contamination levels and state assessment in the lakes of the Oliveri-Tindari Lagoon (North-Eastern Sicily, Italy). *Chem. Ecol.* **2009**, *25*, 27–38. [CrossRef]
29. Ruta, M.; Pepi, M.; Gaggi, C.; Bernardini, E.; Focardi, S.; Magaldi, E.; Gasperini, S.; Volterrani, M.; Zanini, A.; Focardi, S.E. As (V)-reduction to as (III) by arsenic-resistant *Bacillus* spp. bacterial strains isolated from low-contaminated sediments of the Oliveri-Tindari Lagoon, Italy. *Chem. Ecol.* **2011**, *27*, 207–219. [CrossRef]
30. Atzori, P.; Cirrincione, R.; Kern, H.; Mazzoleni, P.; Pezzino, A.; Pugliesi, G.; Pasturo, R.; Trombetta, A. The abundance of 53 elements and petrovolumetric models of the crust in North-Eastern Peloritani mountains (Site 8). *Rend. Lincei* **2003**, *22*, 309–358.
31. Signa, G.; Tramati, C.D.; Vizzini, S. Contamination by trace metals and their trophic transfer to the biota in a Mediterranean coastal system affected by gull guano. *Mar. Ecol. Prog. Ser.* **2013**, *479*, 13–24. [CrossRef]
32. Ryther, J.H.; Guillard, R.R.L. Studies of marine planktonic diatoms: II. Use of *Cyclotella nana* Hustedt for assays of vitamin B12 in sea water. *Can. J. Microbiol.* **1962**, *8*, 437–445. [CrossRef]
33. Sánchez, C.; Cristóbal, G.; Bueno, G. Diatom identification including life cycle stages through morphological and texture descriptors. *PeerJ* **2019**, *7*, e6770. [CrossRef]
34. Yuan, J.; Li, M.; Lin, S. An improved DNA extraction method for efficient and quantitative recovery of phytoplankton diversity in natural assemblages. *PLoS ONE* **2015**, *10*, e0133060. [CrossRef] [PubMed]
35. Ballesteros, I.; Terán, P.; Guamán-Burneo, C.; González, N.; Cruz, A.; Castillejo, P. DNA barcoding approach to characterize microalgae isolated from freshwater systems in Ecuador. *Neotrop. Biodivers.* **2021**, *7*, 170–183. [CrossRef]
36. Lee, S.R.; Oak, J.H.; Chung, I.K.; Lee, J.A. Effective molecular examination of eukaryotic plankton species diversity in environmental seawater using environmental PCR, PCR-RFLP, and sequencing. *J. Appl. Phycol.* **2010**, *22*, 699–707. [CrossRef]
37. Tong, C.Y.; Lew, J.K.; Derek, C.J.C. Algal extracellular organic matter pre-treatment enhances microalgal biofilm adhesion onto microporous substrate. *Chemosphere* **2022**, *307*, 135740. [CrossRef] [PubMed]
38. Abramoff, M.D.; Magelhaes, P.J.; Ram, S.J. Image processing with Image. *J. Biophotonics Int.* **2004**, *11*, 36–42.
39. Zecher, K.; Jagmann, N.; Seemann, P.; Philipp, B. An efficient screening method for the isolation of heterotrophic bacteria influencing growth of diatoms under photoautotrophic conditions. *J. Microbiol. Methods* **2015**, *119*, 154–162. [CrossRef]
40. Jeffrey, S.T.; Humphrey, G.F. New spectrophotometric equations for determining chlorophylls *a*, *b*, *c*1 and *c*2 in higher plants, algae and natural phytoplankton. *Biochem. Physiol. Pflanz.* **1975**, *167*, 191–194. [CrossRef]
41. Prieto-Barajas, C.M.; Valencia-Cantero, E.; Santoyo, G. Microbial mat ecosystems: Structure types, functional diversity, and biotechnological application. *Electron. J. Biotechnol.* **2018**, *31*, 48–56. [CrossRef]
42. Barral-Fraga, L.; Barral, M.T.; MacNeill, K.L.; Martiñá-Prieto, D.; Morin, S.; Rodríguez-Castro, M.C.; Tuulaikhuu, B.-A.; Guasch, H. Biotic and abiotic factors influencing arsenic biogeochemistry and toxicity in fluvial ecosystems: A review. *Int. J. Environ. Res. Public Health* **2020**, *17*, 2331. [CrossRef]
43. Bhosle, N.B.; Subhash, S.S.; Garg, A.; Wagh, A.B.; Evans, L.V. Chemical characterization of exopolysaccharides from the marine fouling diatom *Amphora coffeaeformis*. *Biofouling* **1996**, *10*, 301–307. [CrossRef]

44. Mitbavkar, S.; Anil, A.C. Diatoms of the microphytobenthic community in a tropical intertidal sand flat influenced by monsoons: Spatial and temporal variations. *Mar. Biol.* **2006**, *148*, 693–709. [CrossRef]
45. Mitbavkar, S.; Anil, A.C. Species interactions within a fouling diatom community: Roles of nutrients, initial inoculum and competitive strategies. *Biofouling* **2007**, *23*, 99–112. [CrossRef] [PubMed]
46. Stratton, G.W.; Corke, C.T. The effect of cadmium ions on the growth, photosynthesis and nitrogen activity of *Anabaena inaequalis*. *Can. J. Microbiol.* **1979**, *25*, 1094–1099. [CrossRef] [PubMed]
47. Singh, A.K.; Rai, L.C. Cr and Hg toxicity assessed *in situ* using the structural and functional-characteristics of algal communities. *Environ. Toxicol. Water Qual.* **1991**, *6*, 97–107. [CrossRef]
48. Anantharaj, K.; Govindasamy, C.; Natanamurugaraj, G.; Jeyachandran, S. Effect of heavy metals on marine diatom *Amphora coffeaeformis* (Agardh. Kutz). *Glob. J. Environ. Res.* **2011**, *5*, 112–117.
49. Naveed, S.; Li, C.; Zhang, J.; Zhang, C.; Ge, Y. Sorption and transformation of arsenic by extracellular polymeric substances extracted from *Synechocystis* sp. PCC6803. *Ecotoxicol. Environ. Saf.* **2020**, *206*, 111200. [CrossRef]
50. Chow, S.; Lee, C.; Engel, A. The influence of extracellular polysaccharides, growth rate, and free coccoliths on the coagulation efficiency of *Emiliania huxleyi*. *Mar. Chem.* **2015**, *175*, 5–17. [CrossRef]
51. Leandro, S.M.; Gil, M.C.; Delgadillo, I. Partial characterisation of exopolysaccharides exudated by planktonic diatoms maintained in batch cultures. *Acta Oecol.* **2003**, *24*, 49–55. [CrossRef]
52. Zhang, S.; Xu, C.; Santschi, P.H. Chemical composition and 234Th (IV) binding of extracellular polymeric substances (EPS) produced by the marine diatom *Amphora* sp. *Mar. Chem.* **2008**, *112*, 81–92. [CrossRef]
53. Coste, M.; Boutry, S.; Tison-Rosebery, J.; Delmas, F. Improvements of the Biological Diatom Index (BDI): Description and efficiency of the new version (BDI-2006). *Ecol. Indic.* **2009**, *9*, 621–650. [CrossRef]
54. Rodríguez-Castro, M.C.; Urrea, G.; Guasch, H. Influence of the interaction between phosphate and arsenate on periphyton's growth and its nutrient uptake capacity. *Sci. Total Environ.* **2015**, *503*, 122–132. [CrossRef] [PubMed]
55. Mekkawy, I.A.; Mahmoud, U.M.; Moneeb, R.H.; Sayed, A.E.D.H. Significance assessment of *Amphora coffeaeformis* in arsenic-induced hemato-biochemical alterations of African catfish (*Clarias gariepinus*). *Front. Mar. Sci.* **2020**, *7*, 191. [CrossRef]